2018

Isolation, evaluation of bioactivity and structure determination of amethinol A, a prototypic amethane diterpene from Isodon amethystoides bearing a six/five/seven-membered carbon-ring system

Chen-Liang Zhao
Guiyang University of Chinese Medicine, Guiyang, China

Md. Shahid Sarwar
School of Chinese Medicine, Hong Kong Baptist University

Jiang-Hai Ye
Guiyang University of Chinese Medicine, Guiyang, China

Chuen Fai Ku
School of Chinese Medicine, Hong Kong Baptist University

Wan-Fe Li
School of Chinese Medicine, Hong Kong Baptist University

STRUCTURAL CHEMISTRY

ISSN: 2053-2296
journals.iucr.org/c

Isolation, evaluation of bioactivity and structure determination of amethinol A, a prototypic amethane diterpene from *Isodon amethystoides* bearing a six/five/seven-membered carbon-ring system

Chen-Liang Zhao, Md. Shahid Sarwar, Jiang-Hai Ye, Chuen Fai Ku, Wan-Fei Li, Guo-Yong Luo, Jing-Jie Zhang, Jun Xu, Zhao-Feng Huang, Siu Wai Tsang, Lu-Tai Pan and Hong-Jie Zhang

Acta Cryst. (2018). C**74**, 635–640

Acta Cryst C STRUCTURAL CHEMISTRY
ISSN 2053-2296

Isolation, evaluation of bioactivity and structure determination of amethinol A, a prototypic amethane diterpene from *Isodon amethystoides* bearing a six/five/seven-membered carbon-ring system

Received 7 March 2018
Accepted 12 April 2018

Edited by V. Langer, Chalmers University of Technology, Sweden

‡ Chen-Liang Zhao and Md. Shahid Sarwar contributed equally to this work.

Keywords: *Isodon amethystoides*; Lamiaceae; amethane diterpene; amethinol A; RORγt antagonist; crystal structure; natural product; biosynthetic pathway.

CCDC reference: 1520907

Supporting information: this article has supporting information at journals.iucr.org/c

Chen-Liang Zhao,[a]‡ Md. Shahid Sarwar,[b]‡ Jiang-Hai Ye,[a] Chuen Fai Ku,[b] Wan-Fei Li,[b] Guo-Yong Luo,[a] Jing-Jie Zhang,[a] Jun Xu,[a] Zhao-Feng Huang,[c] Siu Wai Tsang,[b] Lu-Tai Pan[a]* and Hong-Jie Zhang[b]*

[a]Guiyang University of Chinese Medicine, Guiyang 550002, People's Republic of China, [b]School of Chinese Medicine, Hong Kong Baptist University, Hong Kong SAR, People's Republic of China, and [c]Institute of Human Virology, Zhongshan school of Medicine, Sun Yat-sen University, Guangzhou 510080, People's Republic of China. *Correspondence e-mail: ltpan@sina.cn, zhanghj@hkbu.edu.hk

We report the isolation of a novel diterpene, designated as 'amethane', from *Isodon amethystoides* (Lamiaceae). The diterpene [amethinol A; systematic name: (4a*R*,4b*R*,7*R*,10a*S*)-4b,7-dihydroxy-7-isopropyl-1,1-dimethyl-9-oxododecahydrobenzo[*a*]azulene-4a(2*H*)-carboxylic acid], possesses a unique skeleton containing a six/five/seven-membered tricyclic system. Intermolecular O—H···O close contacts were found to the carboxyl, carbonyl and hydroxy groups, connecting molecules into a two-dimensional structure. A possible biosynthetic pathway has been proposed. In addition, the compound was evaluated for its biological activities against different disease targets, and was found to significantly attenuate RORγt-dependent autoimmune responses.

1. Introduction

Chemical constituents and biological activities of *Isodon* plants have been the subjects of continuous studies for decades (Lazarski *et al.*, 2014; Sun *et al.*, 2006; Wang *et al.*, 2011). *ent*-Kaurene diterpenoids are the major focus of the bioactive compounds in the genus (Lu *et al.*, 2013; Riehl *et al.*, 2015). In our recent studies, we have discovered several novel types of non-*ent*-kaurene diterpenes from the *Isodon* genus. For example, rubesanolides A and C were two novel abietanes isolated from *I. rubescens*, with the former containing a unique β-lactone subgroup formed between positions C-9 and C-20 (Zou *et al.*, 2011), and the latter containing a rare γ-lactone subgroup formed between positions C-8 and C-20 (Zou *et al.*, 2012). Some of these also possess good biological activities, an example being fladin A, which is a novel pimarane diterpenoid obtained from *I. flavidus* showing antifungal potential against the athlete's foot fungus (Li *et al.*, 2016).

The genus *Isodon* is distributed all around China, particularly in the southwest provinces (Wu & Li, 1977). Many *Isodon* plants have been used as traditional Chinese medicines (Chen *et al.*, 1996) and *I. amethystoides* is one of them. The plant, known as 'wangzaozi' in Chinese, has been used as a folk medicine to treat pneumonia, pharyngitis and sore throat by the Shui minority of Guizhou Province (Wu, 1977). Previous phytochemical studies on this species revealed that the structures of the diterpenoids differed with respect to region.

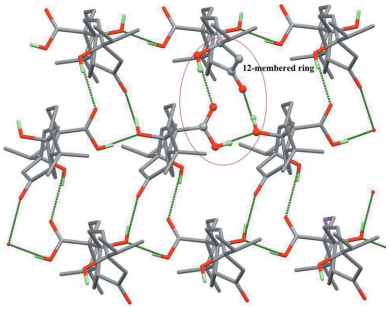

For example, umbrosins A and B and 14-acetylumbrosin B were isolated from the plant collected in Henan province (Li *et al.*, 1981). Amethystiodin A was abundantly found in the plant native to Jiangsu province (Cheng *et al.*, 1982). Meanwhile, wangzaozi A, glaucocalyxins A and B and rabdosinatol were obtained from the plant collected in Anhui province (Wang *et al.*, 1982, 1994).

Based on the folk medicine information of *I. amethystoides*, we investigated the chemical constituents of the stems and leaves found in Guizhou Province. We have since discovered a novel diterpenoid, which we designated as amethinol A, (**1**). Spectroscopic and X-ray crystallographic analyses determined that (**1**) represents an unprecedented diterpenoid with a novel six/five/seven-membered carbon skeleton (see Scheme). This article describes the isolation, structure elucidation, including absolute stereochemistry, and hypothetical biogenetic pathway of (**1**), in addition to its biological activities.

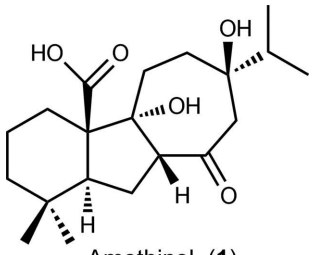

Amethinol, (**1**)

2. Experimental

2.1. Isolation, crystallization, data collection and structure deduction

The leaves and stems of *I. amethystoides* were collected in Libo, Guizhou province, People's Republic of China, in September of 2014. The plant species was authenticated by Professor Junhua Zhao of the Guiyang College of Traditional Chinese Medicine. The air-dried and powdered raw material (32.4 kg) was extracted with MeOH (90 l × 4) at room temperature to give a crude extract (6.1 kg), which was subjected to silica-gel column separation, eluting with a gradient solvent system of petroleum ether/EtOAc (1:0–0:1 *v*/*v*) to yield six fractions (I–VI). Fraction III was further separated by silica-gel column chromatography, Sephadex LH-20 and semipreparative HPLC (Agilent 1100) to afford compound (**1**) (10.5 mg) as a white soild. The molecular formula ($C_{20}H_{32}O_5$) was established by analysis of the ^{13}C NMR and DEPT (distortionless enhancement by polarization transfer) spectra, and confirmed on the basis of the HR–ESI–MS at *m*/*z* 351.2185 $[M - H]^-$ (calculated for $C_{20}H_{31}O_5$, 351.2177). The ^{13}C NMR, DEPT-135 and DEPT-90 spectra of (**1**) (Table 1) exhibited 20 carbon signals, characterized as four non-oxymethyl carbons (δ_C 15–35 ppm), seven non-oxymethylene carbons (δ_C 20–55 ppm), three non-oxymethine carbons (δ_C 43.1, 53.0 and 60.9 ppm), two tertiary oxy-carbons (δ_C 73.5 and 83.8 ppm), two quaternary carbons (δ_C 34.3 and 63.0 ppm), one carboxylic carbon (δ_C 178.8 ppm) and one ketone carbonyl carbon (δ_C 210.7 ppm).

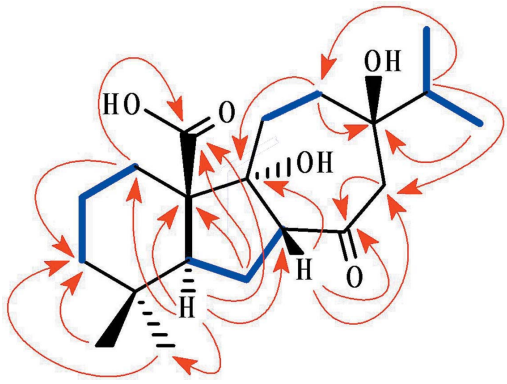

Figure 1
Key ^1H–^1H COSY (bold in blue) and HMBC (arrow in red) correlations of (**1**).

More conclusive structural information could be obtained by analysis of the correlation information provided by the ^1H–^1H COSY (correlation spectroscopy), HSQC (heteronuclear single quantum coherence) and HMBC (heteronuclear multiple bond correlation) spectral data of compound (**1**) (Fig. 1). In the ^1H–^1H COSY spectrum, four individual spin systems were deduced to correspond to four substructure units [*i.e.* $-CH_2-CH_2-CH_2-$, $-CH-CH_2-CH-$, $-CH_2-CH_2-$ and $-CH(CH_3)_2$], which, along with the two methyl signals at δ_H 0.93 and 1.11 ppm, could be used as the starting points for elucidation of the chemical structure of (**1**).

The $-CH_2-CH_2-CH_2-$ segment was determined due to the presence of the methylene correlation signals between the protons at δ_H 2.66/1.88 ppm and the protons at δ_H 2.22/1.74 ppm, and between the protons at δ_H 2.22/1.74 ppm and the protons at δ_H 1.20/1.44 ppm. The $-CH-CH_2-CH-$ segment was elucidated due to the presence of the correlation signals between the methine proton at δ_H 2.59 ppm and the methylene protons at δ_H 3.05/2.57 ppm, and between the methylene protons at δ_H 3.05/2.57 ppm and the methine proton at δ_H 5.05 ppm. The $-CH_2-CH_2-$ segment was deduced due to the presence of the methylene correlation signals between the protons at δ_H 2.93/2.38 ppm and the protons at δ_H 2.48/1.90 ppm. The $-CH(CH_3)_2$ segment was determined due to the presence of the correlation signals between the methine proton at δ_H 1.84 ppm and the two methyl protons at δ_H 1.01/0.99 ppm, and this segment was further connected to a tertiary oxy carbon to yield a $-C(OH)-CH(CH_3)_2$ substructure by the presence of the HMBC correlation of the proton signals of the segment to the carbon signal at δ_C 73.5 ppm.

Through further analysis of the C—H long-range correlations in the HMBC spectrum, two additional substructure units were deduced for (**1**). The presence of the correlations of the two methyl protons (δ_H 0.93 and 1.11 ppm) to the quaternary carbon at δ_C 34.3 ppm established the segment structure of $-C(CH_3)_2$. The presence of the correlations of the methylene protons at δ_H 3.23/2.99 ppm to the carbonyl carbon at δ_C 210.7 ppm led to the determination of the segment structure of $-CH_2-C(=O)-$.

The 20 carbons in (**1**) are thus concluded by including the 17 carbons in the six substructure units [*i.e.* $-CH_2-CH_2-CH_2-$,

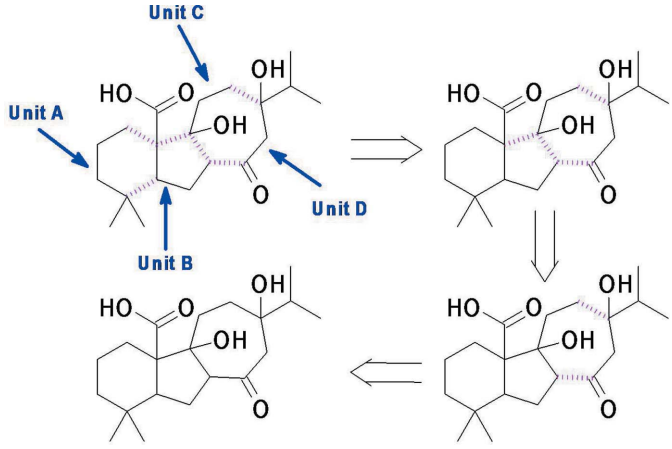

Figure 2
Structure deduction of (**1**). The dotted lines indicate the carbon–carbon bonds that connect the deduced substructures.

–CH–CH_2–CH–, –CH_2–CH_2–, –C(OH)–$CH(CH_3)_2$, –$C(CH_3)_2$ and –CH_2–C(═O)–] elucidated above, the carboxyl carbon, the second quaternary carbon and the second tertiary oxy carbon.

The six substructure units and the functional groups could be connected to one another to afford further substructure units (**Units A–D**) by analyzing the HMBC spectral data of (**1**) (Fig. 2). The presence of the HMBC correlations of the methyl protons at δ_H 0.93 and 1.11 ppm to the methylene carbon at δ_C 42.7 ppm connected the $-C(CH_3)_2$ and $-CH_2-CH_2-CH_2-$ segments to form the $-C(CH_3)_2-CH_2-CH_2-CH_2-$ substructure unit (**Unit A**). The presence of the HMBC correlations of the methine proton at δ_H 2.59 ppm to the carboxyl carbon δ_C 178.8 ppm and the second quaternary carbon at δ_C 63.0 ppm determined the –CH–CH_2–CH–COOH substructure unit (**Unit B**). The presence of the HMBC correlations of the two methylene protons at δ_H 2.93/2.38 and δ_H 2.48/1.90 ppm to the second tertiary oxy carbon at δ_C 83.8 ppm established the –CH_2–CH_2–C–OH substructure unit (**Unit C**). **Unit D** [*i.e.* –C(═O)–CH_2–C(OH)–$CH(CH_3)_2$] was deduced by the observation of the long-range correlations of the methylene protons at δ_H 3.23/2.99 ppm to the tertiary oxy carbon at δ_C 73.5 ppm. The chemical structure of compound (**1**) could thus be elucidated by identification of the HMBC correlations among the four structure units (**Units A–D**).

While the methylene carbon at δ_H 2.66/1.88 ppm of **Unit A** was deduced to be connected to the tertiary carbon of **Unit B** due to the presence of the HMBC correlations of the methylene protons to the quaternary carbon and the carboxylic carbon, the tertiary carbon of **Unit A** was connected to the methine carbon at δ_C 53.0 ppm of **Unit B** due to the presence of the HMBC correlations of the two methyl protons to the methine carbon. The second methine carbon at δ_C 60.9 ppm and the quaternary carbon of **Unit B** were both

Table 1
NMR spectral data (*J* in Hz) of amethinol A, (**1**).

Data were recorded in C_5D_5N on a Varian 400 MHZ spectrometer (^1H, ^{13}C, DEPT, HMBC, HSQC and COSY); chemical shifts (δ values) are given in ppm with reference to the signal of TMS (δ 0 ppm).

Position	δ_H, mult	δ_C, mult
1α	1.88, *br td* (12.9, 3.7)	29.2 CH_2
1β	2.66, *br d* (12.2)	–
2α	1.74, *br d* (13.5)	22.0 CH_2
2β	2.22, *br qt* (13.4, 3.3)	–
3α	1.20, *br td* (13.4, 3.7)	42.7 CH_2
3β	1.44, *br d* (12.8)	–
4	–	34.3 C
5α	2.59, *br d* (10.6)	53.0 CH
6α	3.05, *br dd* (11.1, 3.5)	24.4 CH_2
6β	2.57, *br q* (11.0)	–
7β	5.05, *br dd* (10.8, 4.8)	60.9 CH
8	–	210.7 C
9	–	83.8 C
10	–	63.0 C
11α	2.38, *br dt* (13.7, 2.9)	31.7 CH_2
11β	2.93, *br td* (13.4, 3.7)	–
12α	2.48, *br td* (13.4, 3.7)	32.3 CH_2
12β	1.90, *br dd* (13.0, 3.7)	–
13	–	73.5 C
14α	3.23, *d* (17.6)	52.4 CH_2
14β	2.99, *br d* (17.4)	–
15	1.84, *br septet* (6.8)	43.1 CH
16	0.99, *d*, 3H (6.8)	17.9 CH_3
17	1.01, *d* (6.8)	18.0 CH_3
18	0.93, *s*	32.4 CH_3
19	1.11, *s*	20.8 CH_3
20	–	178.8 C
9-OH	6.36, *br s*	–
13-OH	6.01, *br s*	–

Table 2
Experimental details.

Crystal data	
Chemical formula	$C_{20}H_{32}O_5$
M_r	352.45
Crystal system, space group	Orthorhombic, $P2_12_12_1$
Temperature (K)	170
a, *b*, *c* (Å)	6.4641 (2), 11.6518 (4), 25.4249 (9)
V (Å^3)	1914.96 (11)
Z	4
Radiation type	Cu *K*α
μ (mm^{-1})	0.70
Crystal size (mm)	0.28 × 0.15 × 0.12
Data collection	
Diffractometer	Bruker APEXII CCD
Absorption correction	Multi-scan (*SADABS*; Bruker, 2012)
T_{min}, T_{max}	0.722, 0.786
No. of measured, independent and observed [$I > 2\sigma(I)$] reflections	24714, 3648, 3630
R_{int}	0.032
(sin $\theta/\lambda)_{max}$ (Å^{-1})	0.616
Refinement	
$R[F^2 > 2\sigma(F^2)]$, $wR(F^2)$, *S*	0.028, 0.074, 1.05
No. of reflections	3648
No. of parameters	242
H-atom treatment	H atoms treated by a mixture of independent and constrained refinement
$\Delta\rho_{max}$, $\Delta\rho_{min}$ (e Å^{-3})	0.23, −0.14
Absolute structure	Flack *x* determined using 1495 quotients $[(I^+) - (I^-)]/[(I^+) + (I^-)]$ (Parsons *et al.*, 2013)
Absolute structure parameter	0.04 (3)

Computer programs: *APEX2* (Bruker, 2012), *SAINT* (Bruker, 2012), *SHELXT* (Sheldrick, 2015*a*), *SHELXL2014* (Sheldrick, 2015*b*) and *OLEX2* (Dolomanov *et al.*, 2009).

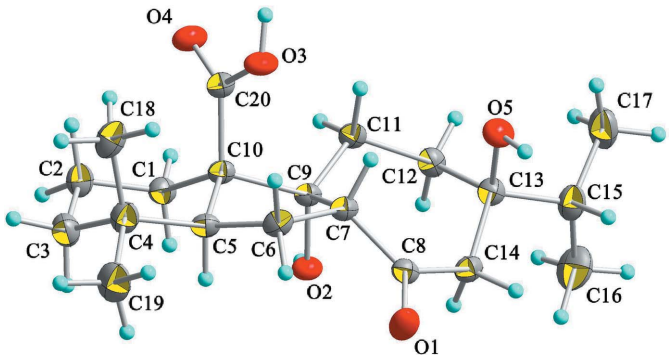

Figure 3
The molecular structure of compound (**1**), showing the atom-numbering scheme. Displacement ellipsoids are drawn at the 50% probability level.

connected to the tertiary oxy carbon of **Unit C** due to the presence of the HMBC correlations of all protons in **Unit B** to the tertiary oxy carbon of **Unit C**. The presence of the HMBC correlations of the methine proton at δ_H 5.05 ppm and the methylene protons in **Unit B** to the carbonyl carbon of **Unit D** connected **Units B** and **D**, and the presence of the HMBC correlations of the two methylene protons of **Unit C** and the tertiary oxy carbon of **Unit D** further connected **Units C** and **D**. We thus obtained the structure of compound (**1**) as shown in Fig. 2 through analysis of the two-dimensional spectral data of the compound. This represents a unique six/five/seven-membered tricyclic diterpene structural skeleton that has not been reported previously. We have designated this type of diterpene structure as 'amethane', and we report compound (**1**) as the first example of the amethanes.

In order to complete the full characterization of (**1**) and to elucidate its absolute configuration, (**1**) was crystallized from methanol to afford crystals suitable for X-ray analysis. The final refinement on the Cu *Kα* data of the crystal of (**1**) resulted in a Flack parameter of 0.04 (3) (Parsons *et al.*, 2013), allowing an unambiguous assignment of the absolute structure of (**1**) (Fig. 3). The five chiral centres C-5, C-7, C-9, C-10 and C-13 were thus determined as *S*, *R*, *R*, *R* and *R*, respectively. Accordingly, the structure of (**1**) was established with a systematic name of (4a*R*,4b*R*,7*R*,10a*S*)-4b,7-dihydroxy-7-isopropyl-1,1-dimethyl-9-oxododecahydrobenzo[*a*]azulene-4a(2*H*)-carboxylic acid, and given the trivial name amethinol A.

2.2. Refinement

Crystal data, data collection and structure refinement details are summarized in Table 2. All the carbon-bound H atoms were generated geometrically and refined using a riding model, with C—H = 0.98–1.00 Å, and with the corresponding U_{iso}(H) values set at 1.5U_{eq}(C) for the methyl groups and at 1.2U_{eq}(C) for the methylene and methenyl groups. The H atoms of the hydroxy groups were located in difference electron-density maps and refined freely.

2.3. Possible biosynthetic pathway

In a previous phytochemical study, lophanic acid (**2**), an abietane diterpene (Wang *et al.*, 1995), was found to be abundant in *I. amethystoides* and is thus considered as a plausible biogenetic precursor of (**1**) (Fig. 4). In the presence of oxygen, the enzyme peroxidase could firstly cleave the C=C double bond of lophanic acid to form a dione (Mutti *et al.*, 2010). The dione intermediate then undergoes an aldol condensation under the enzyme catalyst aldolase to produce amethinol A, (**1**) (Schmidt *et al.*, 2016).

2.4. Bioactivity evaluation

We have investigated the biological activities of amethinol A, (**1**), in various assays. The compound showed no inhibitory activity against cancer cells (HCT116 colorectal and A549 lung), viruses (HIV-1, Ebola and bird flu), dental bacteria (*Streptococcus mutans* and *S. sobrinus*) and the athlete's foot fungus (*Trichophyton rubrum*) at a concentration of 20 μg ml^{-1}. However, (**1**) demonstrated an antagonistic effect against RORγt, a key transcription regulator linked to human autoimmune diseases.

About 70 human diseases, such as lupus nephritis, psoriasis, multiple sclerosis (MS), rheumatoid arthritis (RA), inflammatory bowel disease (IBD) and asthma, are associated with autoimmune disorders, which affect approximately 5% of the world's population (Goodnow *et al.*, 2005). RORγt has been characterized as a principal transcription regulator of Th17 differentiation, which contributes to the pathogenesis of various autoimmune diseases (Ivanov *et al.*, 2006). In this regard, compounds that serve as RORγt antagonists are potential therapeutics for autoimmune disorders. In this study, the effect of (**1**) on RORγt inhibition was assessed in terms of the RORγt-promoter-driven luciferase activity. A Jurkat cell-based reporter assay system was developed in our previous study, which expressed a fusion protein of RORγt LBD with GAL4 DBD and the pGL4.31 reporter gene in the Jurkat cell line (Ding *et al.*, 2015). Upon the addition of (**1**) to RORγt±Jurkat stable cells at 10 μg ml^{-1}, the luciferase

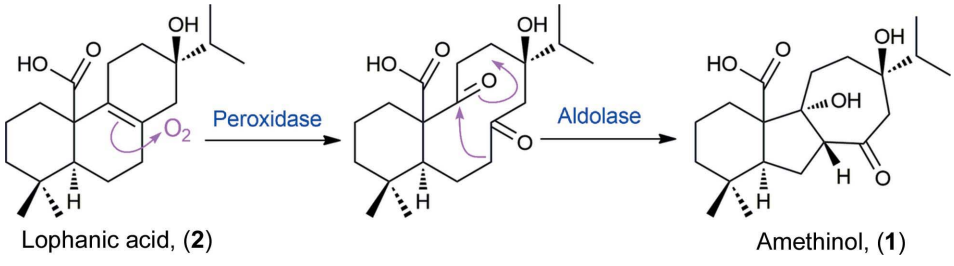

Figure 4
Proposed biosynthetic pathways of compound (**1**).

Table 3
Hydrogen-bond geometry (Å, °).

D—H···A	D—H	H···A	D···A	D—H···A
O2—H2···O1^{i}	0.84 (3)	1.89 (3)	2.7101 (17)	165 (2)
O3—H3···O2^{ii}	0.86 (3)	1.81 (3)	2.6499 (16)	166 (2)
O5—H5···O4^{iii}	0.84 (3)	2.18 (3)	2.9797 (17)	158 (2)

Symmetry codes: (i) $-x+2, y-\frac{1}{2}, -z+\frac{1}{2}$; (ii) $x-1, y, z$; (iii) $-x+1, y+\frac{1}{2}, -z+\frac{1}{2}$.

activity was attenuated by approximately 78%, indicating (**1**) as a potential RORγt inhibitor.

3. Results and discussion

The asymmetric unit of (**1**) consists of one formula unit. As the compound contains only O, C and H atoms, Cu $K\alpha$ radiation was used to enable the determination of the absolute configuration. This corroborated the absolute configuration of the five stereocentres as 5*S*, 7*R*, 9*R*, 10*R* and 13*R*.

Amethinol A, (**1**) is a diterpenoid containing three fused rings. Six-membered ring *A* (atoms C1–C5/C10) has a chair conformation, with atoms C3 and C10 deviating from the best plane through atoms C1/C2/C4/C5 by −0.627 and 0.712 Å, respectively. It is fused through atoms C5 and C10 to five-membered ring *B* (atoms C5–C7/C9–C10), which adopts an envelope conformation on atom C10. In ring *B*, atom C10 deviates by −0.629 Å from the best plane through atoms C5/C6/C7/C9. Moreover, seven-membered ring *C* (atoms C7–C8/C9/C11–C14), fused to ring *B* at atoms C7 and C9, has a twist-chair conformation. This molecule also contains several functional groups. The methyl (C18), carboxyl (C20) and hydroxy (at C13) groups all lie on the β face of the molecule. Only the hydroxy group at C9 and the C19 methyl group are in α positions. There are three crystallographically independent O—H···O hydrogen bonds connecting three adjacent molecules to form a 12-membered ring structure (Table 3 and Fig. 5). In addition, compound (**1**) is expanded into a two-dimensional structure along the crystallographic *a* and *b* directions through these three hydrogen bonds.

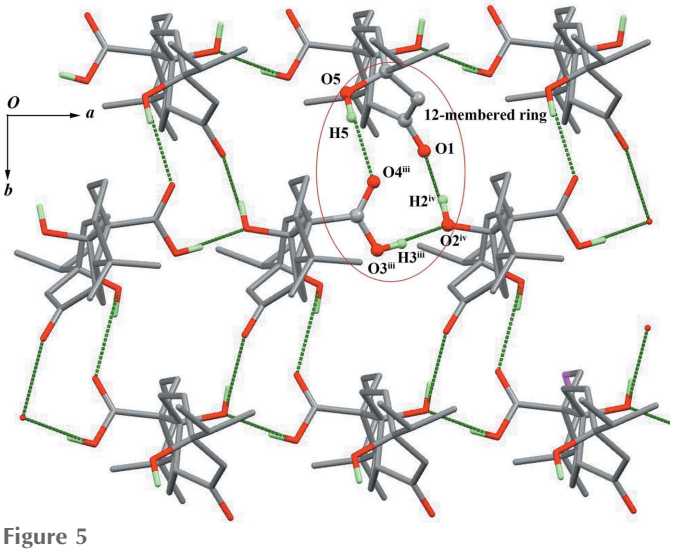

Figure 5
The two-dimensional network structure of compound (**1**). Symmetry-related amethinol molecules are linked through intermolecular hydrogen bonds (dashed lines). All carbon-bound H atoms have been omitted for clarity. [Symmetry codes: (iii) $-x+1, y+\frac{1}{2}, -z+\frac{1}{2}$; (iv) $-x+2, y+\frac{1}{2}, -z+\frac{1}{2}$.]

In summary, amethinol A, (**1**), a novel diterpene with an unprecedented six/five/seven-membered ring carbon skeleton, was identified from the twigs and leaves of *Isodon amethystoides*. The chemical structure was determined by extensive spectroscopic methods. The absolute configuration of (**1**) was confirmed by single-crystal X-ray diffraction analysis using Cu $K\alpha$ radiation. Lophanic acid, a rich chemical constituent found in *Isodon* plants, was proposed as the precursor of (**1**) in its plausible biogenetic pathway. In addition, the attenuation of luciferase activity confirmed (**1**) as an effective RORγt inhibitor.

Funding information

Funding for this research was provided by: National Natural Science Foundation of China (grant No. 81760772); Domestic First-rate Fund of China [grant No. GNYL(2017)008]; Hong Kong Baptist University (HKBU) Interdisciplinary Research Matching Scheme (grant No. RC-IRMS/15-16/02); Science and Technology Department of Guangdong province (grant No. 2016A050503023).

References

Bruker (2012). *APEX2*, *SAINT* and *SADABS*. Bruker AXS Inc., Madison, Wisconsin, USA.
Chen, L. J., Li, Z. H. & Lai, X. P. (1996). *Chin. Med. Mat.* **19**, 169–174.
Cheng, P. Y., Xu, M. J., Lin, Y. L. & Shi, J. C. (1982). *Acta Pharm. Sin.* **17**, 33–37.
Ding, Q. F., Zhao, M., Bai, C., Yu, B. L. & Huang, Z. F. (2015). *BMC Immunol.* **16**, article No. 32.
Dolomanov, O. V., Bourhis, L. J., Gildea, R. J., Howard, J. A. K. & Puschmann, H. (2009). *J. Appl. Cryst.* **42**, 339–341.
Goodnow, C. C., Sprent, J., Fazekas de St Groth, B. & Vinuesa, C. G. (2005). *Nature*, **435**, 590–597.
Ivanov, I. I., McKenzie, B. S., Zhou, L., Tadokoro, C. E., Lepelley, A., Lafaille, J. J., Cua, D. J. & Littman, D. R. (2006). *Cell*, **126**, 1121–1133.
Lazarski, K. E., Moritz, B. J. & Thomson, R. J. (2014). *Angew. Chem. Int. Ed.* **53**, 10588–10599.
Li, J. X., Li, Q. J., Guan, Y. F., Song, X., Liu, Y. H., Zhang, J. J., Li, W. F., Du, J., Zhu, M., Banas, J. A., Li, X. N., Pan, L. T. & Zhang, H. J. (2016). *J. Ethnopharmacol.* **191**, 372–378.
Li, G. Y., Wang, Y. L., Xu, Z. P., Zhang, P. L. & Zhao, W. (1981). *Acta Pharm. Sin.* **16**, 667–671.
Lu, Y., Chen, B., Song, J. H., Zhen, T., Wang, B. Y., Li, X., Liu, P., Yang, X., Zhang, Q. L., Xi, X. D., Chen, S. D., Zuo, J. P., Chen, Z. & Chen, S. J. (2013). *Proc. Natl Acad. Sci. USA*, **110**, 2258–2263.
Mutti, F. G., Lara, M., Kroutil, M. & Kroutil, W. (2010). *Chem. Eur. J.* **16**, 14142–14148.
Parsons, S., Flack, H. D. & Wagner, T. (2013). *Acta Cryst.* B**69**, 249–259.
Riehl, P. S., DePorre, Y. C., Armaly, A. M., Groso, E. J. & Schindler, C. S. (2015). *Tetrahedron*, **71**, 6629–6650.
Schmidt, N. G., Eger, E. & Kroutil, W. (2016). *ACS Catal.* **6**, 4286–4311.
Sheldrick, G. M. (2015*a*). *Acta Cryst.* A**71**, 3–8.
Sheldrick, G. M. (2015*b*). *Acta Cryst.* C**71**, 3–8.
Sun, H. D., Huang, S. X. & Han, Q. B. (2006). *Nat. Prod. Rep.* **23**, 673–698.

Wang, L., Li, D., Wang, C., Zhang, Y. & Xu, J. (2011). *Mini Rev. Med. Chem.* **11**, 910–919.
Wang, X. R., Wang, H. P. & Li, Y. W. (1994). *Chin. Tradit. Herbal Drugs*, **25**, 285–287.
Wang, X. R., Wang, Z. Q., Shi, P. C. & Zhou, B. N. (1982). *Anhui Med. J.* **13**, 12–13.
Wang, Z. Q., Xu, F. W. & Dong, H. Z. (1995). *Nat. Prod. Res. Dev*. **7**, 24–28.
Wu, Z. Y. (1977). In *Flora Yunnanica*. Beijing: Science Press.
Wu, Z. Y. & Li, X. W. (1977). In *Flora Reipublicae Popularis Sinicae*. Beijing: Science Press.
Zou, J., Pan, L. T., Li, Q. J., Pu, J. X., Yao, P., Zhu, M., Banas, J. A., Zhang, H. J. & Sun, H. D. (2012). *Org. Biomol. Chem.* **10**, 5039–5044.
Zou, J., Pan, L. T., Li, Q. J., Zhao, J. H., Pu, J. X., Yao, P., Gong, N. B., Lu, Y., Kondratyuk, T. P., Pezzuto, J. M., Fong, H. H. S., Zhang, H. J. & Sun, H. D. (2011). *Org. Lett.* **13**, 1406–1409.

supporting information

Acta Cryst. (2018). C**74**, 635-640 [https://doi.org/10.1107/S2053229618005740]

Isolation, evaluation of bioactivity and structure determination of amethinol A, a prototypic amethane diterpene from *Isodon amethystoides* bearing a six/five/seven-membered carbon-ring system

Chen-Liang Zhao, Md. Shahid Sarwar, Jiang-Hai Ye, Chuen Fai Ku, Wan-Fei Li, Guo-Yong Luo, Jing-Jie Zhang, Jun Xu, Zhao-Feng Huang, Siu Wai Tsang, Lu-Tai Pan and Hong-Jie Zhang

Computing details

Data collection: *APEX2* (Bruker, 2012); cell refinement: *SAINT* (Bruker, 2012); data reduction: *SAINT* (Bruker, 2012); program(s) used to solve structure: SHELXT (Sheldrick, 2015a); program(s) used to refine structure: *SHELXL2014* (Sheldrick, 2015b); molecular graphics: OLEX2 (Dolomanov *et al.*, 2009); software used to prepare material for publication: OLEX2 (Dolomanov *et al.*, 2009).

(4a*R*,4 b*R*,7*R*,10*aS*)-4 b,7-Dihydroxy-7-isopropyl-1,1-dimethyl-9-oxododecahydrobenzo[*a*]azulene-4a(2*H*)-carboxylic acid

Crystal data

$C_{20}H_{32}O_5$
M_r = 352.45
Orthorhombic, $P2_12_12_1$
a = 6.4641 (2) Å
b = 11.6518 (4) Å
c = 25.4249 (9) Å
V = 1914.96 (11) Å^3
Z = 4
$F(000)$ = 768
D_x = 1.223 Mg m^{-3}
Cu $K\alpha$ radiation, λ = 1.54178 Å
Cell parameters from 3751 reflections
θ = 5.6–48.6°
μ = 0.70 mm^{-1}
T = 170 K
Block, colourless
0.28 × 0.15 × 0.12 mm

Data collection

Bruker APEXII CCD diffractometer
φ and ω scan
Absorption correction: multi-scan (SADABS; Bruker, 2012)
T_{min} = 0.722, T_{max} = 0.786
24714 measured reflections
3648 independent reflections
3630 reflections with $I > 2\sigma(I)$
R_{int} = 0.032
θ_{max} = 71.9°, θ_{min} = 4.2°
h = −7→7
k = −13→12
l = −29→30

Refinement

Refinement on F^2
Least-squares matrix: full
$R[F^2 > 2\sigma(F^2)]$ = 0.028
$wR(F^2)$ = 0.074
S = 1.05
3648 reflections
242 parameters
0 restraints
Hydrogen site location: mixed
H atoms treated by a mixture of independent and constrained refinement

$w = 1/[\sigma^2(F_o^2) + (0.0418P)^2 + 0.3285P]$
where $P = (F_o^2 + 2F_c^2)/3$
$(\Delta/\sigma)_{max} = 0.001$
$\Delta\rho_{max} = 0.23$ e Å^{-3}
$\Delta\rho_{min} = -0.14$ e Å^{-3}

Absolute structure: Flack *x* determined using 1495 quotients [(I+)-(I-)]/[(I+)+(I-)] (Parsons *et al.*, 2013)
Absolute structure parameter: 0.04 (3)

Special details

Geometry. All e.s.d.'s (except the e.s.d. in the dihedral angle between two l.s. planes) are estimated using the full covariance matrix. The cell e.s.d.'s are taken into account individually in the estimation of e.s.d.'s in distances, angles and torsion angles; correlations between e.s.d.'s in cell parameters are only used when they are defined by crystal symmetry. An approximate (isotropic) treatment of cell e.s.d.'s is used for estimating e.s.d.'s involving l.s. planes.

Fractional atomic coordinates and isotropic or equivalent isotropic displacement parameters (Å²)

	x	*y*	*z*	U_{iso}*/U_{eq}
O2	0.94217 (16)	0.28421 (10)	0.28036 (4)	0.0226 (2)
H2	0.963 (4)	0.214 (2)	0.2739 (9)	0.042 (6)*
O3	0.30306 (18)	0.35567 (9)	0.31740 (5)	0.0273 (3)
H3	0.179 (4)	0.335 (2)	0.3103 (9)	0.045 (6)*
O5	0.55585 (18)	0.42514 (10)	0.16027 (5)	0.0284 (3)
H5	0.576 (4)	0.494 (2)	0.1522 (9)	0.048 (7)*
O4	0.31887 (18)	0.17124 (9)	0.33942 (5)	0.0302 (3)
O1	0.9565 (2)	0.57373 (10)	0.25697 (5)	0.0359 (3)
C8	0.8617 (2)	0.49022 (13)	0.24168 (6)	0.0226 (3)
C13	0.7537 (2)	0.36813 (13)	0.15861 (6)	0.0239 (3)
C20	0.4053 (2)	0.26256 (13)	0.33269 (6)	0.0222 (3)
C5	0.7133 (2)	0.38684 (13)	0.36756 (6)	0.0233 (3)
H5A	0.8674	0.3794	0.3681	0.028*
C10	0.6389 (2)	0.27869 (12)	0.33756 (6)	0.0207 (3)
C1	0.7326 (3)	0.17358 (13)	0.36456 (6)	0.0251 (3)
H1A	0.8853	0.1764	0.3617	0.030*
H1B	0.6839	0.1029	0.3468	0.030*
C14	0.9149 (2)	0.44040 (13)	0.18854 (6)	0.0241 (3)
H14A	1.0396	0.3921	0.1931	0.029*
H14B	0.9547	0.5051	0.1654	0.029*
C7	0.6936 (2)	0.43776 (12)	0.27520 (6)	0.0208 (3)
H7	0.5592	0.4508	0.2567	0.025*
C6	0.6729 (3)	0.48890 (13)	0.33102 (6)	0.0247 (3)
H6A	0.7760	0.5504	0.3368	0.030*
H6B	0.5326	0.5206	0.3367	0.030*
C9	0.7232 (2)	0.30567 (12)	0.28054 (6)	0.0195 (3)
C11	0.6197 (2)	0.23782 (13)	0.23618 (6)	0.0226 (3)
H11A	0.4744	0.2638	0.2331	0.027*
H11B	0.6171	0.1558	0.2463	0.027*
C12	0.7222 (3)	0.24793 (13)	0.18195 (6)	0.0250 (3)
H12A	0.6380	0.2031	0.1567	0.030*
H12B	0.8594	0.2105	0.1841	0.030*
C4	0.6520 (3)	0.39262 (15)	0.42607 (6)	0.0302 (4)
C2	0.6694 (3)	0.17070 (15)	0.42285 (7)	0.0319 (4)

H2A	0.5176	0.1608	0.4254	0.038*
H2B	0.7357	0.1041	0.4402	0.038*
C15	0.8242 (3)	0.36049 (15)	0.10016 (6)	0.0325 (4)
H15	0.8295	0.4411	0.0868	0.039*
C3	0.7326 (3)	0.28090 (16)	0.45154 (6)	0.0349 (4)
H3A	0.8855	0.2844	0.4531	0.042*
H3B	0.6808	0.2770	0.4881	0.042*
C18	0.4185 (3)	0.40647 (16)	0.43549 (7)	0.0373 (4)
H18A	0.3671	0.4721	0.4153	0.056*
H18B	0.3930	0.4195	0.4730	0.056*
H18C	0.3466	0.3367	0.4242	0.056*
C19	0.7637 (4)	0.49480 (18)	0.45147 (7)	0.0443 (5)
H19A	0.9117	0.4909	0.4433	0.066*
H19B	0.7445	0.4922	0.4897	0.066*
H19C	0.7064	0.5666	0.4377	0.066*
C17	0.6691 (4)	0.29680 (18)	0.06540 (7)	0.0468 (5)
H17A	0.6767	0.2143	0.0727	0.070*
H17B	0.7020	0.3107	0.0283	0.070*
H17C	0.5290	0.3246	0.0729	0.070*
C16	1.0403 (4)	0.3110 (2)	0.09255 (8)	0.0511 (6)
H16A	1.1410	0.3585	0.1114	0.077*
H16B	1.0744	0.3102	0.0550	0.077*
H16C	1.0445	0.2325	0.1063	0.077*

Atomic displacement parameters (Å²)

	U^{11}	U^{22}	U^{33}	U^{12}	U^{13}	U^{23}
O2	0.0176 (5)	0.0180 (6)	0.0320 (5)	0.0018 (4)	−0.0007 (4)	0.0001 (4)
O3	0.0180 (6)	0.0220 (6)	0.0420 (6)	0.0006 (4)	−0.0023 (5)	0.0025 (4)
O5	0.0272 (6)	0.0225 (6)	0.0354 (6)	0.0028 (5)	−0.0040 (5)	0.0033 (5)
O4	0.0235 (6)	0.0219 (6)	0.0453 (7)	−0.0047 (5)	−0.0011 (5)	0.0043 (5)
O1	0.0467 (7)	0.0299 (6)	0.0311 (6)	−0.0201 (6)	−0.0010 (5)	0.0007 (5)
C8	0.0219 (7)	0.0176 (7)	0.0284 (7)	−0.0004 (6)	−0.0055 (6)	0.0037 (6)
C13	0.0258 (7)	0.0194 (7)	0.0266 (7)	0.0009 (6)	−0.0009 (6)	0.0007 (6)
C20	0.0216 (7)	0.0188 (7)	0.0261 (7)	0.0002 (6)	0.0006 (6)	−0.0008 (6)
C5	0.0209 (7)	0.0216 (7)	0.0276 (8)	−0.0022 (6)	−0.0007 (6)	−0.0020 (6)
C10	0.0194 (7)	0.0166 (7)	0.0262 (7)	−0.0006 (5)	−0.0014 (6)	0.0012 (6)
C1	0.0236 (8)	0.0219 (8)	0.0298 (8)	0.0013 (6)	−0.0019 (6)	0.0038 (6)
C14	0.0241 (7)	0.0192 (7)	0.0290 (7)	−0.0013 (6)	0.0013 (6)	0.0025 (6)
C7	0.0193 (7)	0.0155 (7)	0.0275 (7)	0.0004 (6)	−0.0011 (6)	0.0000 (5)
C6	0.0267 (8)	0.0175 (7)	0.0298 (8)	−0.0018 (6)	0.0025 (6)	−0.0028 (6)
C9	0.0166 (7)	0.0156 (7)	0.0262 (7)	0.0003 (5)	−0.0009 (6)	0.0004 (5)
C11	0.0241 (7)	0.0167 (7)	0.0272 (7)	−0.0020 (6)	−0.0023 (6)	0.0004 (6)
C12	0.0318 (8)	0.0177 (7)	0.0254 (7)	−0.0007 (6)	−0.0031 (6)	−0.0004 (6)
C4	0.0359 (9)	0.0282 (8)	0.0265 (8)	−0.0031 (7)	0.0012 (7)	−0.0015 (6)
C2	0.0362 (9)	0.0284 (9)	0.0311 (8)	0.0010 (7)	−0.0016 (7)	0.0093 (6)
C15	0.0435 (10)	0.0259 (8)	0.0281 (8)	−0.0022 (8)	0.0025 (7)	0.0021 (6)
C3	0.0395 (10)	0.0385 (10)	0.0268 (8)	−0.0007 (8)	−0.0034 (7)	0.0033 (7)

C18	0.0434 (10)	0.0351 (10)	0.0334 (9)	0.0008 (8)	0.0121 (8)	−0.0010 (7)
C19	0.0610 (13)	0.0410 (10)	0.0309 (9)	−0.0094 (10)	0.0001 (9)	−0.0095 (8)
C17	0.0684 (14)	0.0457 (11)	0.0262 (8)	−0.0134 (10)	−0.0033 (9)	−0.0011 (8)
C16	0.0549 (13)	0.0580 (13)	0.0403 (11)	0.0074 (11)	0.0172 (10)	−0.0049 (10)

Geometric parameters (Å, º)

O2—H2	0.84 (3)	C9—C11	1.531 (2)
O2—C9	1.4377 (18)	C11—H11A	0.9900
O3—H3	0.86 (3)	C11—H11B	0.9900
O3—C20	1.3285 (19)	C11—C12	1.534 (2)
O5—H5	0.84 (3)	C12—H12A	0.9900
O5—C13	1.4417 (19)	C12—H12B	0.9900
O4—C20	1.2138 (19)	C4—C3	1.544 (2)
O1—C8	1.214 (2)	C4—C18	1.537 (3)
C8—C14	1.510 (2)	C4—C19	1.535 (3)
C8—C7	1.510 (2)	C2—H2A	0.9900
C13—C14	1.541 (2)	C2—H2B	0.9900
C13—C12	1.535 (2)	C2—C3	1.532 (3)
C13—C15	1.557 (2)	C15—H15	1.0000
C20—C10	1.527 (2)	C15—C17	1.529 (3)
C5—H5A	1.0000	C15—C16	1.523 (3)
C5—C10	1.549 (2)	C3—H3A	0.9900
C5—C6	1.531 (2)	C3—H3B	0.9900
C5—C4	1.541 (2)	C18—H18A	0.9800
C10—C1	1.529 (2)	C18—H18B	0.9800
C10—C9	1.580 (2)	C18—H18C	0.9800
C1—H1A	0.9900	C19—H19A	0.9800
C1—H1B	0.9900	C19—H19B	0.9800
C1—C2	1.538 (2)	C19—H19C	0.9800
C14—H14A	0.9900	C17—H17A	0.9800
C14—H14B	0.9900	C17—H17B	0.9800
C7—H7	1.0000	C17—H17C	0.9800
C7—C6	1.545 (2)	C16—H16A	0.9800
C7—C9	1.557 (2)	C16—H16B	0.9800
C6—H6A	0.9900	C16—H16C	0.9800
C6—H6B	0.9900		

C9—O2—H2	109.0 (17)	C9—C11—C12	115.71 (13)
C20—O3—H3	107.7 (16)	H11A—C11—H11B	107.4
C13—O5—H5	107.4 (18)	C12—C11—H11A	108.4
O1—C8—C14	118.68 (15)	C12—C11—H11B	108.4
O1—C8—C7	120.45 (14)	C13—C12—H12A	107.7
C14—C8—C7	120.88 (13)	C13—C12—H12B	107.7
O5—C13—C14	109.49 (12)	C11—C12—C13	118.36 (13)
O5—C13—C12	106.94 (13)	C11—C12—H12A	107.7
O5—C13—C15	108.30 (13)	C11—C12—H12B	107.7
C14—C13—C15	107.74 (13)	H12A—C12—H12B	107.1

C12—C13—C14	113.42 (13)	C5—C4—C3	106.34 (14)
C12—C13—C15	110.84 (13)	C18—C4—C5	114.05 (14)
O3—C20—C10	114.53 (13)	C18—C4—C3	110.75 (15)
O4—C20—O3	121.89 (14)	C19—C4—C5	108.61 (14)
O4—C20—C10	123.48 (14)	C19—C4—C3	108.59 (15)
C10—C5—H5A	104.2	C19—C4—C18	108.36 (16)
C6—C5—H5A	104.2	C1—C2—H2A	109.3
C6—C5—C10	106.26 (12)	C1—C2—H2B	109.3
C6—C5—C4	120.52 (13)	H2A—C2—H2B	107.9
C4—C5—H5A	104.2	C3—C2—C1	111.69 (14)
C4—C5—C10	115.53 (13)	C3—C2—H2A	109.3
C20—C10—C5	116.55 (12)	C3—C2—H2B	109.3
C20—C10—C1	109.24 (12)	C13—C15—H15	106.3
C20—C10—C9	106.91 (12)	C17—C15—C13	112.79 (15)
C5—C10—C9	100.54 (11)	C17—C15—H15	106.3
C1—C10—C5	107.90 (12)	C16—C15—C13	114.29 (15)
C1—C10—C9	115.77 (12)	C16—C15—H15	106.3
C10—C1—H1A	109.6	C16—C15—C17	110.15 (17)
C10—C1—H1B	109.6	C4—C3—H3A	108.6
C10—C1—C2	110.18 (13)	C4—C3—H3B	108.6
H1A—C1—H1B	108.1	C2—C3—C4	114.65 (14)
C2—C1—H1A	109.6	C2—C3—H3A	108.6
C2—C1—H1B	109.6	C2—C3—H3B	108.6
C8—C14—C13	119.87 (13)	H3A—C3—H3B	107.6
C8—C14—H14A	107.4	C4—C18—H18A	109.5
C8—C14—H14B	107.4	C4—C18—H18B	109.5
C13—C14—H14A	107.4	C4—C18—H18C	109.5
C13—C14—H14B	107.4	H18A—C18—H18B	109.5
H14A—C14—H14B	106.9	H18A—C18—H18C	109.5
C8—C7—H7	107.3	H18B—C18—H18C	109.5
C8—C7—C6	115.14 (13)	C4—C19—H19A	109.5
C8—C7—C9	111.16 (12)	C4—C19—H19B	109.5
C6—C7—H7	107.3	C4—C19—H19C	109.5
C6—C7—C9	108.17 (12)	H19A—C19—H19B	109.5
C9—C7—H7	107.3	H19A—C19—H19C	109.5
C5—C6—C7	104.06 (12)	H19B—C19—H19C	109.5
C5—C6—H6A	110.9	C15—C17—H17A	109.5
C5—C6—H6B	110.9	C15—C17—H17B	109.5
C7—C6—H6A	110.9	C15—C17—H17C	109.5
C7—C6—H6B	110.9	H17A—C17—H17B	109.5
H6A—C6—H6B	109.0	H17A—C17—H17C	109.5
O2—C9—C10	107.92 (12)	H17B—C17—H17C	109.5
O2—C9—C7	107.00 (12)	C15—C16—H16A	109.5
O2—C9—C11	109.75 (12)	C15—C16—H16B	109.5
C7—C9—C10	103.55 (11)	C15—C16—H16C	109.5
C11—C9—C10	115.00 (12)	H16A—C16—H16B	109.5
C11—C9—C7	113.13 (12)	H16A—C16—H16C	109.5
C9—C11—H11A	108.4	H16B—C16—H16C	109.5

C9—C11—H11B	108.4		
O2—C9—C11—C12	−48.56 (17)	C1—C10—C9—C7	−152.65 (13)
O3—C20—C10—C5	47.36 (18)	C1—C10—C9—C11	83.42 (16)
O3—C20—C10—C1	169.94 (12)	C1—C2—C3—C4	54.8 (2)
O3—C20—C10—C9	−64.09 (15)	C14—C8—C7—C6	173.36 (13)
O5—C13—C14—C8	45.65 (18)	C14—C8—C7—C9	49.92 (18)
O5—C13—C12—C11	−52.52 (18)	C14—C13—C12—C11	68.28 (18)
O5—C13—C15—C17	−58.06 (18)	C14—C13—C15—C17	−176.41 (15)
O5—C13—C15—C16	175.10 (15)	C14—C13—C15—C16	56.76 (19)
O4—C20—C10—C5	−136.33 (15)	C7—C8—C14—C13	23.1 (2)
O4—C20—C10—C1	−13.8 (2)	C7—C9—C11—C12	70.86 (17)
O4—C20—C10—C9	112.22 (16)	C6—C5—C10—C20	−73.26 (16)
O1—C8—C14—C13	−156.69 (15)	C6—C5—C10—C1	163.47 (13)
O1—C8—C7—C6	−6.8 (2)	C6—C5—C10—C9	41.81 (15)
O1—C8—C7—C9	−130.28 (15)	C6—C5—C4—C3	−175.00 (15)
C8—C7—C6—C5	−119.38 (14)	C6—C5—C4—C18	62.6 (2)
C8—C7—C9—O2	33.29 (16)	C6—C5—C4—C19	−58.3 (2)
C8—C7—C9—C10	147.15 (12)	C6—C7—C9—O2	−94.05 (14)
C8—C7—C9—C11	−87.70 (15)	C6—C7—C9—C10	19.82 (15)
C20—C10—C1—C2	−70.13 (17)	C6—C7—C9—C11	144.96 (13)
C20—C10—C9—O2	−161.41 (12)	C9—C10—C1—C2	169.16 (13)
C20—C10—C9—C7	85.39 (13)	C9—C7—C6—C5	5.64 (16)
C20—C10—C9—C11	−38.54 (16)	C9—C11—C12—C13	−55.38 (19)
C5—C10—C1—C2	57.48 (16)	C12—C13—C14—C8	−73.70 (18)
C5—C10—C9—O2	76.47 (13)	C12—C13—C15—C17	58.96 (19)
C5—C10—C9—C7	−36.74 (13)	C12—C13—C15—C16	−67.9 (2)
C5—C10—C9—C11	−160.67 (12)	C4—C5—C10—C20	63.25 (18)
C5—C4—C3—C2	−51.34 (19)	C4—C5—C10—C1	−60.02 (17)
C10—C5—C6—C7	−29.94 (16)	C4—C5—C10—C9	178.32 (13)
C10—C5—C4—C3	55.08 (18)	C4—C5—C6—C7	−163.82 (13)
C10—C5—C4—C18	−67.28 (19)	C15—C13—C14—C8	163.23 (13)
C10—C5—C4—C19	171.78 (14)	C15—C13—C12—C11	−170.37 (14)
C10—C1—C2—C3	−56.66 (19)	C18—C4—C3—C2	73.09 (19)
C10—C9—C11—C12	−170.44 (12)	C19—C4—C3—C2	−168.04 (16)
C1—C10—C9—O2	−39.44 (16)		

Hydrogen-bond geometry (Å, º)

D—H···*A*	*D*—H	H···*A*	*D*···*A*	*D*—H···*A*
O2—H2···O1^{i}	0.84 (3)	1.89 (3)	2.7101 (17)	165 (2)
O3—H3···O2^{ii}	0.86 (3)	1.81 (3)	2.6499 (16)	166 (2)
O5—H5···O4^{iii}	0.84 (3)	2.18 (3)	2.9797 (17)	158 (2)

Symmetry codes: (i) −*x*+2, *y*−1/2, −*z*+1/2; (ii) *x*−1, *y*, *z*; (iii) −*x*+1, *y*+1/2, −*z*+1/2.